Universality of random-site percolation thresholds for two-dimensional complex noncompact neighborhoods

Krzysztof Malarz*

AGH University, Faculty of Physics and Applied Computer Science, al. Mickiewicza 30, 30-059 Kraków, Poland

(Received 4 November 2023; accepted 8 February 2024; published 6 March 2024)

The phenomenon of percolation is one of the core topics in statistical mechanics. It allows one to study the phase transition known in real physical systems only in a purely geometrical way. In this paper, we determine thresholds p_c for random-site percolation in triangular and honeycomb lattices for all available neighborhoods containing sites from the sixth coordination zone. The results obtained (together with the percolation thresholds gathered from the literature also for other complex neighborhoods and also for a square lattice) show the power-law dependence $p_c \propto (\zeta/K)^{-\gamma}$ with $\gamma = 0.526(11)$, 0.5439(63), and 0.5932(47), for a honeycomb, square, and triangular lattice, respectively, and $p_c \propto \zeta^{-\gamma}$ with $\gamma = 0.5546(67)$ independently on the underlying lattice. The index $\zeta = \sum_i z_i r_i$ stands for an average coordination number weighted by distance, that is, depending on the coordination zone number i, the neighborhood coordination number z_i, and the distance r_i to sites in the ith coordination zone from the central site. The number K indicates lattice connectivity, that is, $K = 3$, 4, and 6 for the honeycomb, square, and triangular lattice, respectively.

DOI: 10.1103/PhysRevE.109.034108

I. INTRODUCTION

Percolation [1–4] is one of the core topics in statistical physics as it allows for studying phase transitions and their properties in only a geometrical fashion, i.e., without heating or cooling anything (except for paying unconscionable invoices for electricity in computer centers). Although originating from rheology [5,6] (and still applied there [7]), the applications of percolation theory range from forest fires [8] to disease propagation [9], not omitting problems originating in hard physics (including magnetic [10] and electric [11] properties of solids) but also with implications for nanoengineering [12], materials chemistry [13], agriculture [14], sociology [15], terrorism [16], urbanization [17], dentistry [18], information transfer [19], computer networks [20], the psychology of motivation [21], and finances [22] (see Refs. [23–25] for the most recent reviews also on fractal networks [26] or explosive percolation [27]).

The phase transition mentioned above is first of all characterized by a critical parameter called the *percolation threshold* p_c and much effort went into searching for a universal formula that allows for the prediction p_c based solely on the scalar characteristics of a lattice or a network topology, where the percolation phenomenon occurs. Searching for such dependencies probably is not so different from searching for the alchemic formula for the philosopher's stone—allowing for converting a substance into gold. Such attempts of proposing a universal formula for the percolation threshold were more or less successfully made earlier.

For instance, Galam and Mauger [28] proposed a universal formula,

$$p_c = \frac{p_0}{[(d-1)(z-1)]^a}, \tag{1a}$$

depending on the connectivity of the lattice z and its dimension d. For a site percolation problem they identified two groups of lattices, i.e., two sets of parameters p_0 and a. Their paper was immediately criticized by van der Marck [29,30] who indicated two lattices with identical z and d but different values of p_c associated with these lattices. For two-dimensional lattices the Galam-Mauger formula reduces to

$$p_c = \frac{p_0}{(z-1)^a}, \tag{1b}$$

with $p_0 = 0.8889$ and $a = 0.3601$ for triangular, square, and honeycomb lattices [28]. Their studies were extended to anisotropic lattices without equivalent nearest neighbors, non-Bravais lattices with two atom unit cells, and quasicrystals which required the substitution of z in Eq. (1) by an effective (noninteger) value z_{eff} [31,32].

Very recently, Xun *et al.* [33] in extensive numerical simulations showed that all Archimedean lattices (uniform tilings, i.e., lattices built of repeatable sequences of tails of regular polygons able to cover a two-dimensional plane) exhibit a simple relation

$$p_c = c_1/z, \tag{2a}$$

which due to finite-size effects should be modified by a constant term b,

$$p_c = c_2/z - b. \tag{2b}$$

For example, for the square lattice and extended compact neighborhoods, these constants are $c_2 = 4.527$ and $b = 3.341$ [34]. In two dimensions, for Archimedean lattices up to the tenth coordination zone [33], correlations are also seen by plotting

$$z \text{ vs } -1/\ln(1-p_c). \tag{3}$$

*malarz@agh.edu.pl

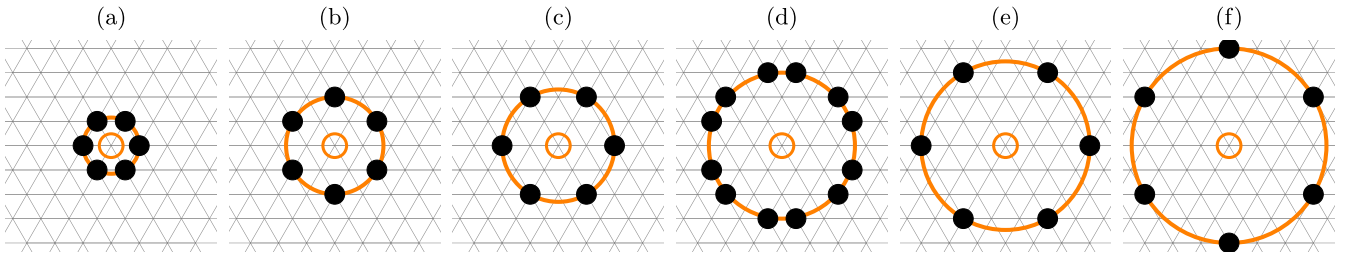

FIG. 1. Basic neighborhoods corresponding to subsequent coordination zones $i = 1, \ldots, 6$ in the triangular lattice. The symbol r stands for the Euclidean distance of the black sites from the central one, and z indicates the number of sites in the neighborhood. (a) TR-1: $i = 1$, $r^2 = 1$, $z = 6$. (b) TR-2: $i = 2$, $r^2 = 3$, $z = 6$. (c) TR-3: $i = 3$, $r^2 = 4$, $z = 6$. (d) TR-4: $i = 4$, $r^2 = 7$, $z = 12$. (e) TR-5: $i = 5$, $r^2 = 9$, $z = 6$. (f) TR-6: $i = 6$, $r^2 = 12$, $z = 6$.

Other formulas investigated by Galam and Mauger [35,36] included

$$p_c = 1/\sqrt{z-1}, \tag{4}$$

or by Koza *et al.* [37,38],

$$p_c = 1 - \exp(d/z). \tag{5}$$

Formula (2a) also works well for distorted lattices [39,40], where lattice distortion means the random moving of lattice nodes not too far from their regular position in nondistorted lattices. In this case, the number of sites in the neighborhood z should be replaced by an average site degree $\bar{z}$ [41].

The studies mentioned above were concentrated in compact neighborhoods. When holes in the neighborhoods are taken into account, there is a strong degeneration of p_c on total z, and Eqs. (1) to (5)—which depend solely on the lattice dimension d and connectivity z—must fail. To avoid this $p_c(z)$ degeneracy in the case of a triangular lattice, a weighted square distance

$$\xi = \sum_i r_i^2 z_i / i \tag{6}$$

was proposed, where z_i is the number of sites in the given neighborhood in the ith coordination zone and these sites' distance to the central site in the neighborhood is r_i [42]. Unfortunately, the clear dependence

$$p_c \propto \xi^{-\gamma} \tag{7}$$

[with $\gamma_{\mathrm{TR}}^{\xi} \approx 0.710(19)$] is lost for the honeycomb lattice [43]. Thus, instead, the weighted coordination number

$$\zeta = \sum_i z_i r_i \tag{8}$$

was proposed [43], which gives a nice power law

$$p_c \propto \zeta^{-\gamma}, \tag{9}$$

with $\gamma_{\mathrm{HC}}^{\zeta} \approx 0.4981(90)$. As $\gamma_{\mathrm{HC}}^{\zeta}$ is very close to $\frac{1}{2}$ also the dependence

$$p_c = c_3/\sqrt{\zeta} \tag{10}$$

was checked, yielding $c_3 \approx 1.2251(99)$ [43]. Very recently, we tested formulas (7) and (9) also for the square lattice up to the sixth coordination zone and found that Eq. (9) also holds for a square lattice with $\gamma_{\mathrm{SQ}}^{\zeta} \approx 0.5454(60)$ [44].

Our results show that for all three (square, triangular, and honeycomb) lattice shapes, the power law is recovered in dependence of $p_c(\zeta/K)$, where K is the connectivity of the network with the nearest-neighbor interaction, that is, with $K = 3$, 4, and 6 for the honeycomb, square, and triangular lattice, respectively. On the other hand, independent of the lattice topology, we see a more or less clear power law $p_c(\zeta)$ for the data obtained on the values of p_c for the three lattices with complex neighborhoods containing sites up to the sixth coordination zone.

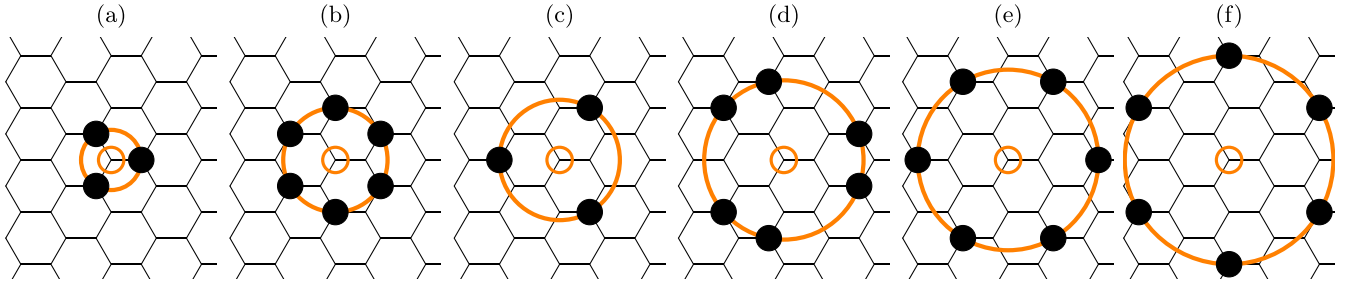

FIG. 2. Basic neighborhoods corresponding to subsequent coordination zones $i = 1, \ldots, 6$ on the honeycomb lattice. The symbol r stands for the Euclidean distance of the black sites from the central one, and z indicates the number of sites in the neighborhood. (a) HC-1: $i = 1$, $r^2 = 1$, $z = 3$. The lattices (b) HC-2 ($i = 2$, $r^2 = 3$, $z = 6$), (e) HC-5 ($i = 5$, $r^2 = 9$, $z = 6$), and (f) HC-6 ($i = 6$, $r^2 = 12$, $z = 6$) are equivalent to a triangular lattice TR-1 [Fig. 1(a)] with enlarged lattice constants $\sqrt{3}$, 3, and $2\sqrt{3}$ times, respectively. (d) HC-4: $i = 4$, $r^2 = 7$, $z = 6$. The lattice (c) HC-3 ($i = 3$, $r^2 = 4$, $z = 3$) is equivalent to HC-1 [Fig. 2(a)] with a lattice constant twice larger than for HC-1.

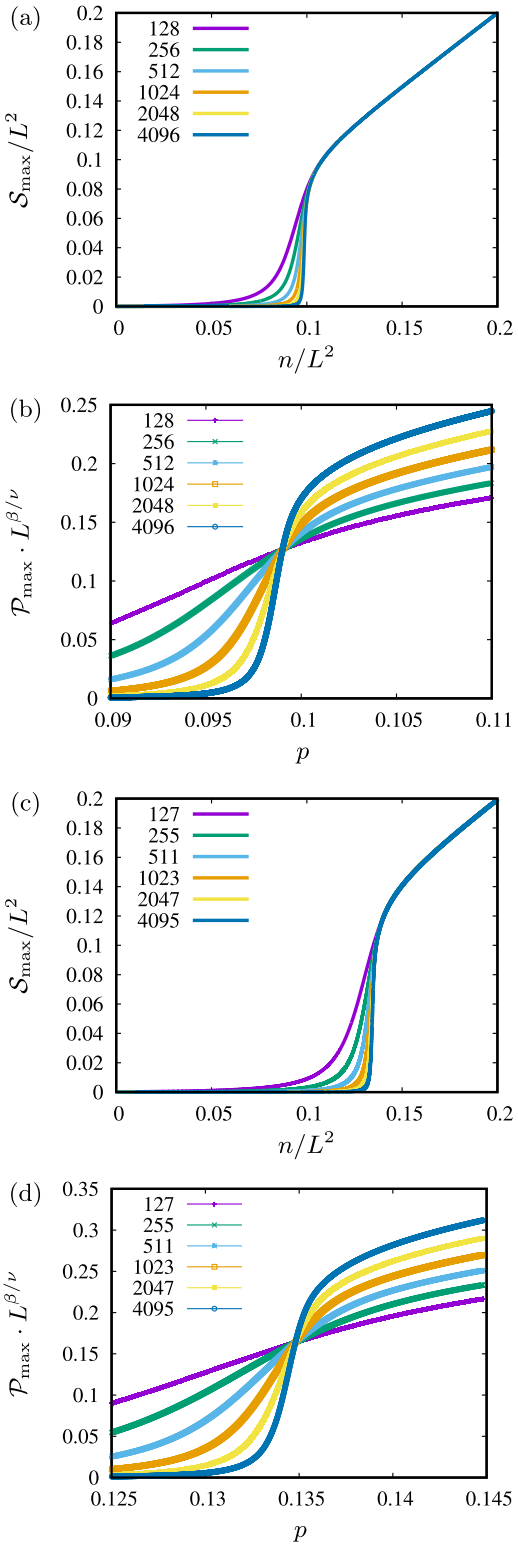

FIG. 3. Examples of (a), (c) $\mathcal{S}_{\max}/L^2$ vs n/L^2 and (b), (d) $\mathcal{P}_{\max} \cdot L^{\beta/\nu}$ vs p for (a), (b) TR-1,2,3,4,5,6 and (c), (d) HC-1,2,3,4,5,6 neighborhoods.

II. METHODOLOGY

In this paper—using exactly the same methodology as that used to study percolation in a square lattice with complex neighborhoods that contain sites up to the sixth coordination zone [44]—we extend our previous studies for sites up to the sixth coordination zone for triangular (Fig. 1) and honeycomb (Fig. 2) lattices. Namely, using the fast Monte Carlo scheme proposed by Newman and Ziff [45] and the finite-size scaling theory [46,47] we found 64 values of percolation thresholds for complex neighborhoods containing sites from the sixth coordination zone.

In the Supplemental Material [48] the mapping of the sixth coordination zone in the honeycomb lattice into the brick-wall-like square lattice (as proposed in Ref. [49]) is presented in Fig. 1 in Supplemental Material App. A together with listing 1 (for the TR-6 neighborhood) and listing 2 (for HC-6 neighborhood) showing implementations of the boundaries() functions to be replaced in the original Newman-Ziff algorithm [45]. The mapping of the first to fifth coordination zones in the honeycomb lattice into the brick-wall-like square lattice is presented in Fig. 3 in Ref. [43].

TABLE I. Detected inflated (together with the associated ζ index) and equivalent neighborhoods. The percolation thresholds p_c and total number of sites z are common for both neighborhoods.

Inflated neighborhood	ζ	p_c	z	Equivalent neighborhood
SQ-2	5.6568	0.5927	4	SQ-1
SQ-3	8	0.5927	4	SQ-1
SQ-5	11.3137	0.5927	4	SQ-1
SQ-6	12	0.5927	4	SQ-1
SQ-2,3	13.6568	0.4073	8	SQ-1,2
SQ-2,5	16.9705	0.337	8	SQ-1,3
SQ-3,5	19.3137	0.4073	8	SQ-1,2
SQ-2,3,5	24.9705	0.288	12	SQ-1,2,3
TR-2	10.3923	0.5	6	TR-1
TR-3	12	0.5	6	TR-1
TR-5	18	0.5	6	TR-1
TR-6	20.7846	0.5	6	TR-1
TR-2,5	28.3923	0.29028	12	TR-1,2
TR-2,6	31.1769	0.26455	12	TR-1,3
TR-3,6	32.7846	0.29030	12	TR-1,2
TR-5,6	38.7846	0.23200	12	TR-2,3
TR-2,5,6	49.1769	0.21550	18	TR-1,2,3
HC-2	10.3923	0.5	6	TR-1
HC-3	6	0.697	3	HC-1
HC-5	15.5884	0.5	6	TR-1
HC-6	20.7846	0.5	6	TR-1
HC-2,5	28.3923	0.29028	12	TR-1,2
HC-2,6	31.1769	0.26453	12	TR-1,3
HC-3,6	26.7846	0.36301	9	HC-1,2
HC-5,6	38.7846	0.23202	12	TR-2,3
HC-2,5,6	49.1769	0.21547	18	TR-1,2,3

III. RESULTS

In Fig. 3 we present examples of results used to predict the percolation thresholds p_c, that is, (i) the dependencies of the size of the largest cluster $\mathcal{S}_{\max}/L^2$ normalized to the lattice size versus the number of occupied sites also normalized to the lattice size [Figs. 3(a) and 3(c)] (ii) the dependencies of the probability that a randomly selected site belongs to the

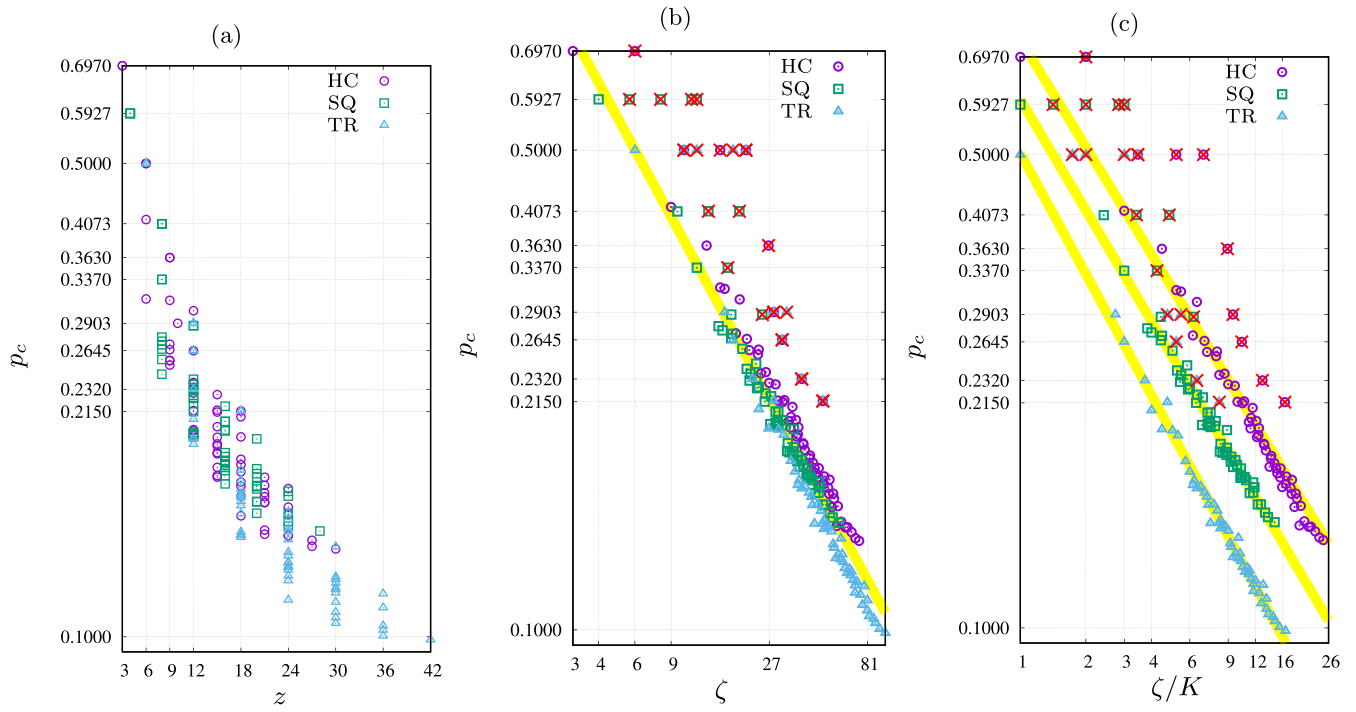

FIG. 4. Percolation thresholds p_c for neighborhoods containing sites up to the sixth coordination zone on square (□), honeycomb (◯), and triangular (△) lattices as dependent on (a) total coordination number z, (b) index ζ, and (c) index ζ/K. Points marked with crosses (×) correspond to inflated neighborhoods (such as those collected in Table I), which are excluded from the fitting procedure. The lines show power-law fits according to the least-squares method to Eq. (9) and Eq. (11) on Figs. 4(b) and 4(c), respectively.

largest cluster, scaled by $L^{\beta/\nu}$ [50] versus occupation probability p [Figs. 3(b) and 3(d)] for triangular [Figs. 3(a) and 3(b) honeycomb [Figs. 3(c) and 3(d)] lattices and neighborhoods containing all considered basic neighborhoods presented in Fig. 1 (for the triangular lattice) and Fig. 2 (for the honeycomb lattice). The linear sizes L of the simulated systems range from 127 to 4096 and the results of these simulations are averaged over $R = 10^5$ samples. All dependencies $\mathcal{P}_{\max} \cdot L^{\beta/\nu}$ vs p studied here are presented in Fig. 2 (for the triangular lattice) and Fig. 3 (for the honeycomb lattice) in Supplemental Material App. C [48]. The common point of the curves $\mathcal{P}_{\max} \cdot L^{\beta/\nu}$ vs p for various system sizes L predicts p_c. The computed values of p_c, associated with various neighborhoods, together with their uncertainties (also estimated earlier for neighborhoods containing sites up to the sixth coordination zone—for a square lattice [44,51,52] and the fifth coordination zone—for triangular [42,53] and honeycomb [43] lattices) are collected in Table I in Supplemental Material App. B [48].

Figure 4 presents the p_c for neighborhoods containing sites up to the sixth coordination zone on square (□), honeycomb (◯), and triangular (△) lattices as dependent on (i) total coordination number z [Fig. 4(a)], (ii) index ζ [Fig. 4(b)], and (iii) index ζ/K [Fig. 4(c)].

The crosses (×) indicate inflated neighborhoods, that is, noncompact neighborhoods reducible to other complex neighborhoods by shrinking the lattice constants. Three examples of inflated neighborhoods are presented in Fig. 5. The detected inflated neighborhoods and their lower-index equivalents are presented in Table I. These values p_c are excluded from the fitting procedure. As we mentioned in the Introduction, for complex noncompact neighborhoods, strong $p_c(z)$ degeneration is observed [see Fig. 4(a)]. On the contrary, introducing the index ζ (8) allows a nearly perfect separation of the values of p_c. After excluding inflated neighborhoods (presented in Table I) the linear fit of the data presented in Fig. 4(c) with the

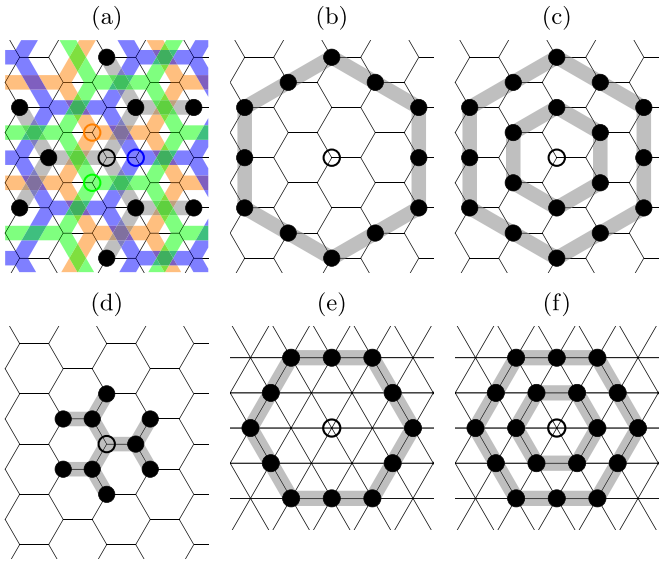

FIG. 5. Inflated complex neighborhoods (top row) and their lower-index partners (bottom row): (a) HC-3,6 vs (d) HC-1,2, (b) HC-5,6 vs (e) TR-2,3, and (c) HC-2,5,6 vs (f) TR-1,2,3. The neighborhood HC-3,6 is equivalent to HC-1,2 but with a lattice constant twice as large. This splits the system into four independent simultaneously percolating systems.

least-squares method gives in the power law

$$p_c \propto (\zeta/K)^{-\gamma} \tag{11}$$

exponents $\gamma_{\mathrm{TR}} = 0.5932(47)$, $\gamma_{\mathrm{SQ}} = 0.5439(63)$, $\gamma_{\mathrm{HC}} = 0.526(11)$, for triangular, square, and honeycomb lattices, respectively. The analogous fit according to Eq. (9) of the data presented in Fig. 4(b) gives the exponent $\gamma_{\mathrm{2D}} = 0.5546(67)$.

IV. DISCUSSION

The introduction of the ζ index solves the problem of multiple degeneration of the value of p_c. Eliminating inflated neighborhoods (including those that occur pairwise between a triangular and a hexagonal lattice) allows fitting p_c to the power laws according to Eqs. (9) or (11). Without comparing the hexagonal and triangular lattices, it was necessary to introduce the index ξ to maintain the power-law relationship according to Eq. (7). The index ξ turned out to be redundant versus ζ index for the site percolation problem, because previously outlier points turned out to belong to the inflated neighborhoods, but the low-index neighborhoods associated with them were located on a different type of lattice. However, the introduction of the index ξ turned out to be quite useful for the bond percolation problem, where the relationship (7) is perfectly satisfied with the exponent $\gamma \approx 1$ [54].

Finally, we propose some unification of the nomenclature appearing in the literature, and applying terms: (1) *basic neighborhoods* for those containing sites from a single coordination zone (such as SQ-1, SQ-2, SQ-3, etc., and those presented in Figs. 1 and 2); (2) *complex neighborhoods* for any combination of the basic ones; (3) *extended neighborhoods* for complex and compact neighborhoods (such as SQ-1,2, TR-1,2,3, HC-1,2,3,4, etc.); and (4) *inflated neighborhoods* for complex neighborhoods reducible to other complex neighborhoods but with lower indices by shrinking the lattice constant (such as those presented in Fig. 5 and collected in Table I).

In conclusion, in this paper we estimate percolation thresholds for the random-site percolation problem on triangular and honeycomb lattices for neighborhoods containing sites from the sixth coordination zone. The obtained values of p_c satisfy the power law, independently of the underlying lattice (according to $p_c \propto \zeta^{-\gamma}$) or even better for separately considered lattices [according to $p_c \propto (\zeta/K)^{-\gamma}$, where K is the connectivity of the lattice]. Currently, the applications of complex neighborhoods on various lattice topologies seem to be most promising in agroecology [14].

ACKNOWLEDGMENTS

The authors thank H. Skawina for preparing the figures for Table I in Supplemental Material App. B [48]. We gratefully acknowledge Poland's high-performance computing infrastructure PLGrid (HPC Center: ACK Cyfronet AGH) for providing computer facilities and support within computational Grant No. PLG/2023/016295.

[1] D. Stauffer and A. Aharony, *Introduction to Percolation Theory*, 2nd ed. (Taylor and Francis, London, 1994).

[2] B. Bollobás and O. Riordan, *Percolation* (Cambridge University Press, Cambridge, UK, 2006).

[3] M. Sahimi, *Applications of Percolation Theory* (Taylor and Francis, London, 1994).

[4] H. Kesten, *Percolation Theory for Mathematicians* (Brikhauser, Boston, 1982).

[5] S. R. Broadbent and J. M. Hammersley, Percolation processes: I. Crystals and mazes, Math. Proc. Cambridge Philos. Soc. **53**, 629 (1957).

[6] J. M. Hammersley, Percolation processes: II. The connective constant, Math. Proc. Cambridge Philos. Soc. **53**, 642 (1957).

[7] D. Soto-Gomez, L. Vazquez Juiz, P. Perez-Rodriguez, J. Eugenio Lopez-Periago, M. Paradelo, and J. Koestel, Percolation theory applied to soil tomography, Geoderma **357**, 113959 (2020); S. F. Bolandtaba and A. Skauge, Network modeling of EOR processes: A combined invasion percolation and dynamic model for mobilization of trapped oil, Transp. Porous Media **89**, 357 (2011); S. C. Mun, M. Kim, K. Prakashan, H. J. Jung, Y. Son, and O. O. Park, A new approach to determine rheological percolation of carbon nanotubes in microstructured polymer matrices, Carbon **67**, 64 (2014); B. Ghanbarian, F. Liang, and H.-H. Liu, Modeling gas relative permeability in shales and tight porous rocks, Fuel **272**, 117686 (2020).

[8] K. Malarz, S. Kaczanowska, and K. Kułakowski, Are forest fires predictable? Int. J. Mod. Phys. C **13**, 1017 (2002); N. Guisoni, E. S. Loscar, and E. V. Albano, Phase diagram and critical behavior of a forest-fire model in a gradient of immunity, Phys. Rev. E **83**, 011125 (2011); A. Simeoni, P. Salinesi, and F. Morandini, Physical modelling of forest fire spreading through heterogeneous fuel beds, Int. J. Wildland Fire **20**, 625 (2011); G. Camelo-Neto and S. Coutinho, Forest-fire model with resistant trees, J. Stat. Mech: Theory Exp. (2011) P06018; S. R. Abades, A. Gaxiola, and P. A. Marquet, Fire, percolation thresholds and the savanna forest transition: A neutral model approach, J. Ecol. **102**, 1386 (2014).

[9] R. M. Ziff, Percolation and the pandemic, Physica A **568**, 125723 (2021).

[10] B. G. Ueland, N. H. Jo, A. Sapkota, W. Tian, M. Masters, H. Hodovanets, S. S. Downing, C. Schmidt, R. J. McQueeney, S. L. Bud'ko, A. Kreyssig, P. C. Canfield, and A. I. Goldman, Reduction of the ordered magnetic moment and its relationship to Kondo coherence in $Ce_{1-x}La_xCu_2Ge_2$, Phys. Rev. B **97**, 165121 (2018); L. Keeney, C. Downing, M. Schmidt, M. E. Pemble, V. Nicolosi, and R. W. Whatmore, Direct atomic scale determination of magnetic ion partition in a room temperature multiferroic material, Sci. Rep. **7**, 1737 (2017); P. Buczek, L. M. Sandratskii, N. Buczek, S. Thomas, G. Vignale, and A. Ernst, Magnons in disordered nonstoichiometric low-dimensional magnets, Phys. Rev. B **94**, 054407 (2016); Y. Yiu, P. Bonfá, S. Sanna, R. De Renzi, P. Carretta, M. A. McGuire, A. Huq, and S. E. Nagler, Tuning the magnetic and structural phase transitions of PrFeAsO via Fe/Ru spin dilution, *ibid.* **90**, 064515 (2014); M. Grady, Possible new phase transition in the 3D Ising model associated with boundary percolation, J. Phys.: Condens. Matter **35**, 285401 (2023).

[11] J. Jeong, K. J. Park, E.-J. Cho, H.-J. Noh, S. B. Kim, and H.-D. Kim, Electronic structure change of $NiS_{2-x}Se_x$ in the

metal-insulator transition probed by x-ray absorption spectroscopy, J. Korean Phys. Soc. **72**, 111 (2018); A. Avella, A. M. Oles, and P. Horsch, Defect-induced orbital polarization and collapse of orbital order in doped vanadium perovskites, Phys. Rev. Lett. **122**, 127206 (2019); L. Cheng, P. Yan, X. Yang, H. Zou, H. Yang, and H. Liang, High conductivity, percolation behavior and dielectric relaxation of hybrid ZIF-8/CNT composites, J. Alloys Compd. **825**, 154132 (2020).

[12] F. Xu, Z. Xu, and B. I. Yakobson, Site-percolation threshold of carbon nanotube fibers—Fast inspection of percolation with Markov stochastic theory, Physica A **407**, 341 (2014).

[13] M. Alguero, M. Perez-Cerdan, R. P. del Real, J. Ricote, and A. Castro, Novel Aurivillius $Bi_4Ti_{3-2x}Nb_xFe_xO_{12}$ phases with increasing magnetic-cation fraction until percolation: A novel approach for room temperature multiferroism, J. Mater. Chem. C **8**, 12457 (2020); M. Meloni, M. J. Large, J. M. González Domínguez, S. Victor-Román, G. Fratta, E. Istif, O. Tomes, J. P. Salvage, C. P. Ewels, M. Pelaez-Fernandez, R. Arenal, A. Benito, W. K. Maser, A. A. K. King, P. M. Ajayan, S. P. Ogilvie, and A. B. Dalton, Explosive percolation yields highly-conductive polymer nanocomposites, Nat. Commun. **13**, 6872 (2022).

[14] J. E. Ramírez, C. Pajares, M. I. Martínez, R. Rodríguez Fernández, E. Molina-Gayosso, J. Lozada-Lechuga, and A. Fernández Téllez, Site-bond percolation solution to preventing the propagation of *Phytophthora* zoospores on plantations, Phys. Rev. E **101**, 032301 (2020); D. R. Herrera, J. Velázquez-Castro, A. F. Téllez, J. F. López-Olguín, and J. E. Ramírez, Site percolation threshold of composite square lattices and its agroecology applications, *ibid.* **109**, 014304 (2024).

[15] A. Moreira, J. Andrade, and D. Stauffer, Sznajd social model on square lattice with correlated percolation, Int. J. Mod. Phys. C **12**, 39 (2001).

[16] S. Galam, The September 11 attack: A percolation of individual passive support, Eur. Phys. J. B **26**, 269 (2002); S. Galam and A. Mauger, On reducing terrorism power: A hint from physics, Physica A **323**, 695 (2003).

[17] W. Cao, L. Dong, L. Wu, and Y. Liu, Quantifying urban areas with multi-source data based on percolation theory, Remote Sens. Environ. **241**, 111730 (2020).

[18] M. Beddoe, T. Gölz, M. Barkey, E. Bau, M. Godejohann, S. A. Maier, F. Keilmann, M. Moldovan, D. Prodan, N. Ilie, and A. Tittl, Probing the micro- and nanoscopic properties of dental materials using infrared spectroscopy: A proof-of-principle study, Acta Biomater. **168**, 309 (2023).

[19] L. Cirigliano, C. Castellano, and G. Timár, Extended-range percolation in complex networks, Phys. Rev. E **108**, 044304 (2023).

[20] G. Liu, Y. Deng, and K. H. Cheong, Network immunization strategy by eliminating fringe nodes: A percolation perspective, IEEE Trans. Syst. Man. Cybern. **53**, 1862 (2023).

[21] K. Malarz and M. Wołoszyn, Thermal properties of structurally balanced systems on classical random graphs, Chaos **33**, 073115 (2023).

[22] S. Bartolucci, F. Caccioli, and P. Vivo, A percolation model for the emergence of the Bitcoin Lightning Network, Sci. Rep. **10**, 4488 (2020).

[23] A. A. Saberi, Recent advances in percolation theory and its applications, Phys. Rep. **578**, 1 (2015).

[24] M. Li, R.-R. Liu, L. Lü, M.-B. Hu, S. Xu, and Y.-C. Zhang, Percolation on complex networks: Theory and application, Phys. Rep. **907**, 1 (2021).

[25] M. Sahimi, Explosive percolation and its applications, in *Applications of Percolation Theory* (Springer, Cham, 2023), pp. 517–548.

[26] M.-A. M. Cruz, J. P. Ortiz, M. P. Ortiz, and A. Balankin, Percolation on fractal networks: A survey, Fractal Fract. **7**, 231 (2023).

[27] Y. Cho and B. Kahng, Discontinuous percolation transitions in cluster merging processes, J. Phys. A: Math. Theor. **55**, 374002 (2022); M. Li, J. Wang, and Y. Deng, Explosive percolation obeys standard finite-size scaling in an event-based ensemble, Phys. Rev. Lett. **130**, 147101 (2023); Q. Wu and J. Wang, Thresholds and critical exponents of explosive bond percolation on the square lattice, Int. J. Mod. Phys. C **33**, 2250096 (2022); Z. Luo, W. Chen, and J. Nagler, Universality of explosive percolation under product and sum rule, Phys. Rev. E **108**, 034108 (2023); K. Hagiwara and Y. Ozeki, Size-independent scaling analysis for explosive percolation, *ibid.* **106**, 054138 (2022).

[28] S. Galam and A. Mauger, Universal formulas for percolation thresholds, Phys. Rev. E **53**, 2177 (1996).

[29] S. C. van der Marck, Comment on "Universal formulas for percolation thresholds", Phys. Rev. E **55**, 1228 (1997).

[30] S. Galam and A. Mauger, Reply to "Comment on 'Universal formulas for percolation thresholds"', Phys. Rev. E **55**, 1230 (1997).

[31] S. Galam and A. Mauger, Universal formulas for percolation thresholds. II. Extension to anisotropic and aperiodic lattices, Phys. Rev. E **56**, 322 (1997).

[32] F. Babalievski, Comment on "Universal formulas for percolation thresholds. II. Extension to anisotropic and aperiodic lattices", Phys. Rev. E **59**, 1278 (1999).

[33] Z. Xun, D. Hao, and R. M. Ziff, Site and bond percolation thresholds on regular lattices with compact extended-range neighborhoods in two and three dimensions, Phys. Rev. E **105**, 024105 (2022).

[34] Z. Xun, D. Hao, and R. M. Ziff, Site percolation on square and simple cubic lattices with extended neighborhoods and their continuum limit, Phys. Rev. E **103**, 022126 (2021).

[35] S. Galam and A. Mauger, A new scheme to percolation thresholds, J. Appl. Phys. **75**, 5526 (1994).

[36] S. Galam and A. Mauger, Site percolation thresholds in all dimensions, Physica A **205**, 502 (1994).

[37] Z. Koza, G. Kondrat, and K. Suszczyński, Percolation of overlapping squares or cubes on a lattice, J. Stat. Mech.: Theory Exp. (2014) P11005.

[38] Z. Koza and J. Poła, From discrete to continuous percolation in dimensions 3 to 7, J. Stat. Mech.: Theory Exp. (2016) 103206.

[39] S. Mitra, D. Saha, and A. Sensharma, Percolation in a distorted square lattice, Phys. Rev. E **99**, 012117 (2019).

[40] S. Mitra, D. Saha, and A. Sensharma, Percolation in a simple cubic lattice with distortion, Phys. Rev. E **106**, 034109 (2022).

[41] S. Mitra and A. Sensharma, Site percolation in distorted square and simple cubic lattices with flexible number of neighbors, Phys. Rev. E **107**, 064127 (2023).

[42] K. Malarz, Percolation thresholds on triangular lattice for neighborhoods containing sites up to the fifth coordination zone, Phys. Rev. E **103**, 052107 (2021).

[43] K. Malarz, Random site percolation on honeycomb lattices with complex neighborhoods, Chaos **32**, 083123 (2022).

[44] K. Malarz, Random site percolation thresholds on square lattice for complex neighborhoods containing sites up to the sixth coordination zone, Physica A **632**, 129347 (2023).

[45] M. E. J. Newman and R. M. Ziff, Fast Monte Carlo algorithm for site or bond percolation, Phys. Rev. E **64**, 016706 (2001).

[46] V. Privman, Finite-size scaling theory, in *Finite Size Scaling and Numerical Simulation of Statistical Systems*, edited by V. Privman (World Scientific, Singapore, 1990), pp. 1–98.

[47] D. P. Landau and K. Binder, *A Guide to Monte Carlo Simulations in Statistical Physics*, 3rd ed. (Cambridge University Press, Cambridge, UK, 2009).

[48] See Supplemental Material at http://link.aps.org/supplemental/10.1103/PhysRevE.109.034108 for (A) the mapping of the sixth coordination zone in the honeycomb lattice, into the brick-wall-like square lattice, together with their implementations in (C); (B) shapes of neighborhoods and associated percolation thresholds; and (C) scaled probability of belonging to the largest cluster versus occupation probability.

[49] P. N. Suding and R. M. Ziff, Site percolation thresholds for Archimedean lattices, Phys. Rev. E **60**, 275 (1999).

[50] For the problem of site percolation, the critical values of the exponents $\beta = \frac{5}{36}$ and $\nu = \frac{4}{3}$ are known exactly (see p. 54 in Ref. [1]).

[51] S. Galam and K. Malarz, Restoring site percolation on damaged square lattices, Phys. Rev. E **72**, 027103 (2005).

[52] M. Majewski and K. Malarz, Square lattice site percolation thresholds for complex neighbourhoods, Acta Phys. Pol., B **38**, 2191 (2007).

[53] K. Malarz, Site percolation thresholds on triangular lattice with complex neighborhoods, Chaos **30**, 123123 (2020).

[54] Z. Xun and D. Hao, Monte Carlo simulation of bond percolation on square lattice with complex neighborhoods, Acta Phys. Sin. **71**, 066401 (2022).